Article:
Dew, L., English, W., Chong, C. et al. (1 more author) (2016) Investigating neovascularization in rat decellularized intestine - an in vitro platform for studying angiogenesis. Tissue Engineering - Part A, 22 (22-23). pp. 1317-1326. ISSN 1937-3368

https://doi.org/10.1089/ten.TEA.2016.0131

Investigating neovascularization in rat decellularized intestine - an in vitro platform for studying angiogenesis

Lindsey Dew[1], William R. English[2], Chuh K. Chong[1] and Sheila MacNeil[1*]

[1]Kroto Research Institute, University of Sheffield, Broad Lane, Sheffield S3 7HQ, UK.
[2]Department of Oncology and Metabolism, School of Medicine, Beech Hill Road, Sheffield S10 2RX, UK.

[*]Corresponding author: Email: s.macneil@sheffield.ac.uk. Kroto Research Institute, University of Sheffield, Broad Lane, Sheffield S3 7HQ, UK.

Key words: Decellularization; Recellularization; Tissue Engineering; Regenerative Medicine; Angiogenesis.

Abstract

One of the main challenges currently faced by tissue engineers is the loss of tissues post implantation due to delayed neovascularization. Several strategies are under investigation to create vascularized tissue but none have yet overcome this problem. In this study we produced a decellularized natural vascular scaffold from rat intestine to use as an in vitro platform for neovascularization studies for tissue engineered constructs. Decellularization resulted in almost complete (97%) removal of nuclei and DNA, while collagen, glycosaminoglycans and laminin content was preserved. Decellularization did, however, result in the loss of elastin and fibronectin. Some pro-angiogenic factors were retained, as fragments of decellularized intestine were able to stimulate angiogenesis in the chick chorioallantoic membrane assay. We demonstrated that decellularization left perfusable vascular channels intact, and these could be re-populated with human dermal microvascular endothelial cells. Optimization of re-endothelialisation of the vascular channels showed this was improved by continuous perfusion of the vasculature and further improved by infusion of human dermal fibroblasts into the intestinal lumen, from where they invaded into the decellularized tissue. Finally we explored the ability of the perfused cells to form new vessels. In the absence of exogenous angiogenic stimuli, Dll4, a marker of endothelial capillary-tip cell activation during sprouting angiogenesis was absent, indicating the reformed vasculature was largely quiescent. However, after addition of VEGFA, Dll4 positive endothelial cells could be detected, demonstrating this engineered vascular construct maintained its capacity for neovascularization. In summary we have demonstrated how a natural xenobiotic vasculature can be used as an in vitro model platform to study

neovascularization and provide information on factors that are critical for efficient re-endothelialisation of decellularized tissue.

Introduction

Tissue engineered constructs are produced to replace damaged, injured or missing tissues through combining materials technology and biotechnology [1, 2]. While significant progress has been made over the last 30 years, one of the major obstacles in the field is the difficulty in achieving rapid neovascularisation when implanting tissues greater than 2mm in thickness [3]. When a tissue-engineered (TE) construct is implanted in vivo the transplanted cells require a supply of oxygen to survive. Oxygen diffusion is often the limiting factor in the ability of cells to survive and as a result few can tolerate being a distance of more than 200μm away from a blood vessel [4, 5]. Unfortunately complete vascularization of TE constructs upon transplantation can take weeks to occur and during this time, the construct cells will become depleted of oxygen and other nutrients leading to the starvation of the tissue and failure of the construct [6].

Blood vessel formation is tightly regulated and relies on the chronologically precise adjustment of vessel growth, maturation and suppression of EC growth - all of which are controlled by a large number of factors which influence each other [7-9]. To induce vascularization within TE substitutes these same processes will need to occur and neovascularization takes time to occur. The complexity of these tightly regulated processes explains why this remains one of the major obstacles in the field of tissue engineering at present. To overcome this, our aim is to firstly to understand and then translate the basic principles of angiogenesis to produce a physiologically relevant TE construct fit for use in the clinic. In order to study the physiological angiogenic environment it would be a major advantage to have an in vitro model that can be used to explore the range of variables (cell types, pro-angiogenic stimuli and perfusion rate)

that simulate the natural microenvironment. Decellularization is an established technique for producing scaffolds that retain the architecture of the original tissue including the vasculature and essential biofactors [10, 11]. We suggest that this is an ideal method to form a perfusable scaffold with intrinsic vasculature that can be repopulated with vascular cells surrounded by ECM components to model angiogenesis. Accordingly the aim of this work was to generate an acellular natural matrix from rat intestine, repopulate this with vascular and stromal cells, subject these cells to constant perfusion using a bioreactor system to study the requirements for efficient re-endothelialisation and to see if the development of neovessels could be induced.

Materials and Methods

Organ preparation. All surgical procedures and animal husbandry were carried out in accordance with the UK Home Office guidelines under the Animals (Scientific Procedures) Act 1986 and the local ethics committee. Ten adult DBIX rats were sacrificed by isoflurane inhalation and cervical dislocation. A longitudinal abdominal incision was made to expose the abdominal cavity. The inferior vena cava was cannulated using a 24G cannula (Terumo Medical Products, NJ, USA) and flushed with approximately 20ml of heparin (100U/ml) in PBS to prevent blood clot formation. An 8-10cm long segment of the jejunum of the small intestine was isolated and vessels at the peripheries of the segment were ligated before the section of the small intestine was explanted. The intestinal lumen of the isolated segment was then immediately flushed with PBS, 100U/mL penicillin, 0.1mg/mL streptomycin and amphotericin B

(0.5mg/ml). The superior mesenteric artery (SMA) was then cannulated with a 24G cannula under a dissection microscope (Wild Heerbrugg M 3Z).

Decellularization. The cannula in the SMA of the intestine was attached to a peristaltic pump (Watson-Marlow 200 series, Scientific Laboratory Supplies, UK). dH_2O was continuously perfused through the vessels at a rate of 2.7 ml/min for ~3 hours with the intestine submerged in dH_2O. Subsequently, 1% (v/v) Triton-X 100 with 0.1% (v/v) ammonium hydroxide in dH_2O was perfused through the tissue overnight. Finally dH_2O was circulated for a further 3 hours to remove any residual detergent. The decellularized intestine was then sterilised with 0.1% (v/v) peracetic acid (PA) via the cannula whilst submerged in PA for 3 hours. This was repeated with sterile PBS three times to remove any residual acid and then the tissue was stored submerged in PBS at 4˚C.

Histological analyses. Samples were fixed for 24 hours at 4˚C in 3.7% v/v formalin solution in PBS followed by embedding in paraffin wax and sectioning at 6µm. Tissue sections were stained with Hematoxylin and Eosin (H&E) (Sigma Aldrich), Alcian Blue (Atom Scientific, UK), PicoSirius Red (Sigma Aldrich), modified Verhoeff Van Gieson elastin stain (Accustain, Sigma Aldrich).

Vascular patency. After decellularization 1ml of blue food dye was injected through the SMA of the intestine to determine the patency of the vessels. The vessels were macroscopically visualized and imaged under a dissection microscope (M 3Z, Wild Heerbrugg, Germany). To observe the patency of the vessels microscopically, approximately 1ml FITC-Dextran dissolved in PBS to a final concentration of

100µg/ml (250kDa, Sigma Aldrich) was infused into the intestine and imaged immediately using a Zeiss LSM 510 confocal microscope (Zeiss, UK).

DNA quantification. Fresh or decellularized tissue was macerated, lyophilized and weighed. 100mg of each sample was digested with proteinase K overnight at 56°C. DNA was then isolated using the DNeasy Blood and Tissue kit (Qiagen, Germany) according to the manufacturer's instructions. The amount of DNA present in each sample was measured by determining the absorbance at 260nm using a NanoDrop 1000 (Thermo Scientific).

Collagen quantification. 100mg of lyophilized tissue was digested in 6M hydrochloric acid at 121°C overnight and neutralised with 6M NaOH. Collagen content was measured indirectly by analysis of hydroxyproline content as described previously [12]. Hydroxyproline concentration was then correlated to collagen content by multiplying by a conversion factor of 5.4 according to Rhaleb et al. [13].

GAG quantification. GAG content was analysed using the dimethylmethylene blue (DMB) assay described by Farndale et al. [14]. 100mg lyophilized tissue was digested with 5ml of papain digestion solution containing 150 units of papain, 5mM of L-cysteine hydrochloride, 5mM EDTA dissolved in PBS with calcium and magnesium. Samples were incubated for 48h at 60°C before transferring 40µl into a clear 96 well plate. DMB solution (250µl; 16mg of 1,9 dimethylene blue, 5ml ethanol, 2ml formic acid, 2g sodium formate adjusted to a volume of 1000ml using dH_2O, pH of 3.0) was added to each well and absorbance measured at 520nm using a microtitreplate spectrophotometer.

Chick chorioallantoic membrane (CAM) assay. Fertilised chick eggs (Henry Stewart and Co., Norfolk, UK) were incubated at a constant temperature of 37°C and humidity of 40%. Seven days post fertilization, a small window was cut into the egg shell. Small segments (~1cm in length) of sterilised decellularized intestine or collagen-I gels were placed onto the CAM. The window was sealed using tape and incubated for 7 days. Changes in the CAM vasculature were imaged through the egg shell window using a USB Digitial Microscope (400x, Maplin, UK). The number of blood vessels less than 10µm in diameter growing towards the samples were counted blind by two independent assessors.

Collagen gel preparation. Working on ice, collagen gels (2mg/ml) were prepared by adding 0.2ml rat tail collagen type I (3mg/ml, Life technologies, Gibco, UK) to 0.1ml of (EC) cell growth medium MV. Sterile 1M sodium hydroxide was added drop-wise to neutralize the pH. Supplemented gels were prepared using the same method with the addition of 3µl of human VEGFA (1ng/µl, Sigma Aldrich). The gels were then allowed to set in a 37°C incubator for 30 min.

Recellularization. Vascular structures were re-endothelialized using a combination of proliferating human dermal microvascular endothelial cells (HDMECs) derived from juvenile foreskin (Promocell) and human dermal fibroblasts (HDFs) derived as described previously [15]. Each intestine was flushed with HDMEC growth medium and allowed to warm in an incubator set at 37 °C in a 5% CO_2 atmosphere prior to cell seeding. To recellularize with HDMECs alone, 1.5×10^6 HDMECs were resuspended in 1ml of growth medium and then perfused through the vasculature of the pre-warmed

decellularized intestine. This was incubated overnight. To recellularize the intestine with HDMECs and HDFs within the vascular channels HDMECs were recellularized into the decellularized intestine as described above. This was incubated for at least 3 hours. 1.5 x 10^6 HDFs were then resuspended in 1ml of HDMEC medium and perfused through the vasculature of the decellularized intestine and incubated overnight. To recellularize the intestine with HDMECs within the vascular channels and HDFs within the intestinal lumen, 0.75 x 10^6 HDFs were resuspended in 5 ml of HDMEC medium and perfused through the lumen of the intestine. This was incubated (fully submerged in HDMEC medium) for at least 3 hours. This process was repeated but this time the intestine was flipped onto the reverse side so that the HDFs were perfused onto the opposite surface of the lumen. Again the intestine was incubated for at least 3 hours. 1.5 × 10^6 cells were resuspended in 1 ml of HDMEC growth medium and perfused through the vasculature before incubating overnight. A section of the intestine (from each cell combination) was removed and cultured under static conditions submerged in media whilst the rest was attached to a peristaltic pump (Watson-Marlow 200 series, Scientific Laboratory Supplies, UK) via the cannula and a bespoke Lexan polycarbonate bioreactor containing 70ml of HDMEC growth media. The samples were placed onto a stainless steel grid to raise them to an air liquid interface. Gas exchange was maintained with the use of an air filter attached to a port of the container. Perfusion was initially tested at rates of 2.7 ml/min and then 0.5 and 0.025 ml/min to find the influence of the rate of perfusion on endothelialisation over 24 and 72 hours.

Production of angiogenesis model. HDMECs were perfused via the vascular channels and HDFs were seeded via the intestinal lumen before placing into the bioreactor as described. Six stainless steel rings were then placed on top of the recellularized

intestine. VEGFA collagen gels were prepared as described and 100µl was pipetted into each metal ring. The bioreactor was then sealed and transferred to an incubator where the gels were allowed to set at 37°C for 15 min. The scaffold was then perfused at 0.025 ml/min for 72h. Collagen gels without VEGFA were used as controls.

Immunofluorescence staining of tissue sections. Samples were fixed for 2 h in 4% paraformaldehyde (PFA) w/v in HBSS with Ca^{2+} and Mg^{2+} before dehydrating using graded alcohol washes and embedding in paraffin wax. Sections of 6 µm thickness were cut and mounted on slides. Samples were de-waxed and rehydrated by submerging sequentially in xylene and graded alcohol solutions. Sections were permeabilised using 0.1% (v/v) Triton-X 100 for 20 min and incubated in 7.5% (w/v) bovine serum albumin (BSA) at room temperature (RT) for 60 min, followed by washing once with 1% (w/v) BSA in PBS. Samples were incubated with either polyclonal rabbit anti-laminin primary antibody (1:100 in 1% (w/v) BSA, Abcam, UK) or polyclonal rabbit anti-fibronectin primary antibody (1:1500 in 1% (w/v) BSA, Abcam, UK) at 4°C overnight. Samples were washed 3 times in PBS before incubating with Alexa Fluor™ 488 nm goat anti-rabbit secondary antibody (1:500 in 1% (w/v) BSA, Life Technologies, UK) at RT for 60 min before washing a further 3 times with PBS. Nuclear counterstaining was performed using DAPI by incubating at RT for 20 min and then washing a further three times with PBS. Samples were imaged using a Zeiss LSM 510 confocal microscope (Zeiss, UK) set at 495nm λ_{ex} - 515nm λ_{em} (FITC) and 358nm λ_{ex} - 461nm λ_{em} (DAPI).

Immunofluorescence staining of whole mounted tissue. Samples were fixed in 4% PFA for 20 minutes at RT. Samples were then quenched with 100 mM glycine, washed once

with PBS, and were then blocked for 1 hour with 1% BSA (w/v) at RT. Mouse anti-CD31 (1:20 in 1% BSA (w/v) Dako, UK) and rabbit anti-DLL4 (1:200 in 1% BSA (w/v), Abcam, UK) primary antibodies were added before incubating at RT overnight. The samples were subsequently washed for 2 hours in 1% BSA/0.1% Tween 20 (w/v / v/v), followed by incubation with Alexa Fluor 546 goat anti-mouse IgG secondary antibody (Life Technologies, UK) for 2 hours at RT. Nuclear counterstaining was performed using DAPI by incubating at RT for 20 min. Finally the samples were washed with 1% BSA/1% Tween20 for at least 8 hours with hourly changes of the BSA/Tween20 solution. Samples were imaged using a Zeiss LSM 510 confocal microscope (Zeiss, UK).

Live/Dead Staining. Propidium iodide and Syto 9 (Life Technologies, UK) were diluted in pre-warmed DMEM in the ratio 1:3000 under sterile conditions. Sections of intestine were taken, transferred to a 6 well plate and incubated at 37°C at 5% CO_2 for 20 minutes. Samples were imaged using a Zeiss LSM 510 confocal microscope (Zeiss, UK).

Statistical analysis. Statistics were performed using a two-tailed, unpaired Student's t-test. The significance of the results are denoted by a * symbol (* = $P < 0.05$, ** = $P < 0.01$, *** = $P < 0.001$).

Results

Decellularization efficiency. To decellularize the intestine the vasculature was used as a transport network to continuously perfuse the non-ionic detergent solution containing

Triton-X 100 and ammonium hydroxide for ~24 hours. The rat intestine became macroscopically transparent after this time and showed good preservation of the mesentery (Fig 1A and B). The vascular channels of the decellularized intestine were easily seen macroscopically (Fig 1C). To test the macroscopic patency of the vessels blue food dye was injected, highlighting the intact vascular structures (Fig 1D). Injection of FITC-Dextran showed that microscopic vascular patency was also preserved (Fig 1E).

Characterization of nuclei and extracellular matrix composition after decellularization. In order to characterize the decellularized intestine as a scaffold the retention of cells and extracellular matrix (ECM) was assessed. H&E staining showed the almost complete removal of cells after the decellularization process, as little to no basophilic staining typical of nuclear material remained (Fig 2A). This was confirmed on staining of tissue with DAPI. Quantification of DNA after extraction showed that 97% of DNA was removed after the decellularization process (Figure 2B).

Collagen content was investigated by staining with picosirius red and imaging the samples using brightfield microscopy (Fig 2A). Collagen is stained red and appears to be retained after decellularization. When examined under polarised light, larger collagen fibers (orange/red) were present, whilst smaller reticular fibers (green) were largely absent. Quantification of collagen content using the hydroxyproline assay showed a relative increase in content after decellularization in weight matched samples (Fig 2B).

Alcian blue staining of the fresh and decellularized intestine showed little difference in staining of glycosaminoglycans (GAG) or mucinous polysaccharides (MPS) (Fig 2A) and further analysis via GAG quantification showed that there was no significant

difference in GAG content after the decellularization process (Fig 2B). Van Gieson staining showed the almost complete removal of elastin (blue/black) (Fig 3). Immunofluorescence staining showed the preservation of laminin after the decellularization process, but not fibronectin (Figure 3).

Angiogenic properties of the bioscaffold. To assess the retention of pro-angiogenic properties of the decellularized scaffold, the chick chorioallantoic membrane (CAM) assay was used. Sections of decellularized intestine were placed onto chick membranes along with collagen gels as negative controls 7 days post fertilization and incubated for a further 7 days. An increase in vascular density could be seen in the CAM incubated with decellularized intestine (Fig 4A). Quantification confirmed a significant increase ($P < 0.0001$) in the number of vessels growing towards the decellularized intestine sections compared to the collagen gel control (Fig 4B).

The effect of perfusion rates on recellularization with endothelial cells. To assess the ability of the decellularized intestine to act as a scaffold for vessel reconstruction and development of new vessels, HDMECs were infused within the vascular channels and allowed to attach to the matrix. Using a live-dead (green-red) cell fluorescent stain, confocal microscopy showed HDMEC present 24h after injection with a low proportion of dead cells, however after 3 days in static culture few viable cells remained in the vascular channels compared to perfused channels (Fig 5). To investigate if survival of HDMEC could be improved by perfusion of the vascular channels, HDMECs were initially infused into the scaffolds and were cultured under static conditions or perfused at rates of 2.7 ml/min initially and then at 0.5 ml/min and 0.025 ml/min (with wall shear stress values of 25.40dyne/cm^2, 4.70dyne/cm^2 and 0.24dyne/cm^2 respectively).

The choice of an initial perfusion rate of 2.7 ml/min was based on a study of physiological measurements of flow through first order mesenteric artery branches of rats. This was shown to be 0.3ml/min [16]. To determine the flow to be applied through the SMA the number of branches for each jejunual segment (in this study, 9) was multiplied by this flow rate since the total flow rate through the SMA is equal to the sum of the flow rates through the first order branches. Using this physical law of continuity the initial perfusion flow rate through the vasculature was accordingly selected to be 2.7ml/min.

Further experiments using LIVE/DEAD® analysis and immunostaining for CD31/PECAM-1 (Fig 5) were then undertaken at much lower flow rates of 0.5 and then 0.025 ml/min. Table 1 shows several experiments in which a qualitative assessment of the extent of endothelialisation at two flow rates, 2.7 and 0.025 ml/min, was made. These show that when the lower flow rate of 0.025 ml/min was used there appeared to be slightly more live cells occupying the vascular channels with a more uniform distribution when compared to the 100 times higher flow rate of 2.7ml/min. Under static conditions results were poor. This suggests that HDMECs need some perfusion to survive throughout the vascular network after initial distribution but the actual rate of flow did not appear critical.

Recellularization of the decellularized intestine with human vascular cells and fibroblasts. As mesenchymal cells such as fibroblasts have been shown to support capillary networks in vitro by mimicking pericytes [7], human dermal fibroblasts (HDF) were co-injected into the vascular channels with the HDMEC. Although this did not increase the number of cells present within the vascular channels under static flow conditions, in the presence of flow a greater number of viable cells could be seen,

although cellular coverage of the vasculature did not appear complete (Fig 6) (also summarised in Table1). As it is possible the HDF are unable to re-populate the precise niche previously occupied by other mesenchymal cells such as pericytes when infused via the vascular channels, HDF were then infused via the intestinal lumen. This led to greater cellular coverage of the vascular channel lumen with fewer dead cells (Fig 6).

To further characterise the effects of flow on HDMEC coverage of the vascular channels using the different methods described above, the intestine was stained for the endothelial marker CD31/PECAM-1. As indicated by live-dead staining, HDMEC coverage of the vascular channel after 3 days was significantly improved by the presence of perfusion. In the absence of HDF, the HDMEC did not form a complete monolayer (Fig 7A) and Table 1. When HDMEC and HDF were infused via the vasculature, $CD31^{+VE}$ cell staining was decreased, with a large proportion of the cells retained being $CD31^{-VE}$, suggesting HDF were lining the vascular lumen (Fig 7A). In contrast when HDF were infused via the intestinal lumen, $CD31^{-VE}$ nuclei could be seen throughout the tissue in proximity with the vascular channels, suggesting HDF invasion into the decellularized tissue. However, this also led to an increase in coverage of $CD31^{+VE}$ cells within the vascular channels under flow (Fig 7A). More detailed examination showed the $CD31^{+VE}$ cells had formed a highly confluent HDMEC monolayer (Fig 7B).

We then investigated if the recellularized vascular channels were actively undergoing sprouting angiogenesis by staining for Delta-like ligand 4 (Dll4), a member of the delta-serrate family of ligands that is expressed exclusively in invading capillary tip cells in response to pro-angiogenic growth factor signalling, including via VEGFA and VEGFR2. Dll4 controls capillary sprout morphology and invasion during sprouting angiogenesis via signalling through Notch in following stalk cells to suppress the tip

cell phenotype and is augmented by signalling from stalk cell expression of Jag1 in a highly dynamic process [17-22]. We were unable to detect $Dll4^{+VE}/CD31^{+VE}$ cells in HDMEC vascular channels indicating sprouting angiogenesis is most likely not active (Fig 8). However, by placing collagen-I gels loaded with VEGFA on top of the decellularized intestine to generate a pro-angiogenic growth factor gradient, Dll4 expression could be detected in $CD31^{+VE}$ cells, showing the recellularized vascular channels retain the capacity for sprouting angiogenesis in the presence of appropriate stimuli (Fig 8).

Discussion

Advances in the field of tissue engineering have shown promising steps towards the regeneration of vital tissues and organs including skin [15], bladder [23], urethra [24] and trachea [25]. However one of the main challenges in almost all cases is the lack of rapid vascularization upon transplantation which leads to early graft failure. Without an understanding of the factors that affect blood vessel formation and sprouting it is unlikely that this problem will be solved. Several in vitro angiogenesis assays are available but none combine the ability to include supporting cells (e.g. smooth muscle cells, pericytes or fibroblasts or other stromal cells), the natural ECM and perfusion and the introduction of pro-angiogenic stimuli [26]. In the present study we aimed to develop an **in vitro** model that will allow all four components to be combined. Continuous perfusion of detergent via the vascular tree of the rat intestine allowed for the production of a natural acellular matrix after ~18 hours. Characterization of the resultant matrix showed a 97% removal of cellular material whilst preserving the macro- and ultrastructural components of the native tissue. Dye perfusion showed the

preservation of the native vascular network whilst histology and quantitative assays showed the preservation of both the GAG and collagen ECM components. The collagen component was shown to increase (relative to other components) after decellularization and is believed to be due to the removal of other components such as cellular proteins. Elastin and fibronectin were both shown to reduce after the process. This is broadly similar to other reports of decellularization, with some differences in retention of ECM, notably GAG, Elastin and fibronectin between our studies and those of others [27-28] Differences in ECM retention may be due to both the methodology of decellularization and the type of tissues used and provides an interesting area for further exploration. However, since this study aimed to induce angiogenic sprouting from microvasculature, the loss of elastin was not of major concern since elastin content is important in larger vessels that require elastic recoil but less important in smaller vessels such as capillaries which consist of only the tunica intima. As is well established, fibronectin is present both in the serum used in the medium to perfuse the vasculature and is also produced by fibroblasts (e.g. [29-30] and was also not considered to be a significant factor in our model.

Results from the CAM assay showed the inherent angiogenic effect of the decellularized intestine. This response argues for the preservation of key growth factors that will ultimately affect cell responses once reseeding takes place. Further characterization is required to identify which pro-angiogenic stimuli are retained, but this novel finding suggests decellularized tissue retains some growth factors that can activate angiogenesis in neighboring tissues. This is an important consideration if these decellularised constructs are to be considered for use as a vascular bed to support tissue-engineering applications (outside of the remit of the current study).

In order to produce an in vitro model to investigate angiogenesis, cells were infused through the vasculature to repopulate the acellular matrix. The response of endothelial cells to shear stress is well known, e.g. [31]. Results clearly showed the necessity for perfusion rather than static culture conditions but a qualitative analysis (Table 1) showed that perfusion at 0.025 ml/min was only slightly better than 2.7ml/min for cells to occupy the innate vascular architectures of the scaffold. This suggests that for this in vitro model there is a wide tolerance to flow as two flow rates varying by 100 fold both achieved excellent to good endothelialisation.

Once the patency of the vascular structures and perfusion conditions were ascertained the intestine was recellularized with a co-culture of HDFs and HDMECs. Studies using mature ECs on their own have shown poor results. Cells have failed to survive and proliferate and most importantly to self-assemble into tube-like structures [32]. Improved results have been noted by using a co-culture of HDMECs and fibroblasts [33,34]. Cell proliferation and cell signalling have been improved through the use of co-cultures and it is believed that this is as a result of paracrine signalling mechanisms that promote production of VEGF from fibroblasts and the upregulation of VEGF receptors on HDMECs [32]. The co-culture of cells in the decellularized intestinal scaffold was performed and maintained under both static and perfusion cultures. Again, the necessity of perfusion was highlighted. Further investigations using perfusion conditions showed the reorganization of the HDMECs and HDFs over time. After one day in culture results showed the positioning of HDMECs and HDFs within the vascular structures of the decellularized intestine. After 5 days in culture under perfusion conditions the cells had reorganized themselves and the HDMECs lined the vessels and capillaries.

In the recellularized lung model of Peterson et al, only epithelial and endothelial cells were introduced, and mesenchymal cells that could act as pericytes were absent, which may have contributed to the poorly functioning and leaky vasculature seen in this model [28].

Dll4 is a well characterised marker of sprouting angiogenesis that is expressed in endothelial cells that become the leading 'tip-cell' within quiescent vasculature. Tip cells mediate the invasion of pre-capillary sprouts into the surrounding stroma in response to a diffusion gradient of pro-angiogenic growth factors including VEGFA that activate expression of Dll4, supress proliferation and activate the invasive phenotype. Dll4 directly supresses the invasive tip-cell phenotype in following endothelial 'stalk-cells' via Notch signalling, thus maintaining invading capillary sprout architecture [17-21] .In this study we used immunostaining of Dll4 to detect evidence of activation of endothelial tip-cell selection, and thus active sprouting angiogenesis, within the vasculature and capillaries containing HDMEC. Although the decellularized intestine clearly initially contained pro-angiogenic growth factors that could support angiogenesis in the CAM assay, we could not detect evidence of sprouting angiogenesis in the absence of exogenous VEGFA. This data reinforces the usefulness of our model vascular system for studying angiogenesis in a tissue-engineered construct and may also prove useful for mechanistic studies of sprouting angiogenesis.

This study shows the ability of these cells to reorganize within this matrix and supports its use as a platform technology in which to model cell behaviour within a physiologically relevant and yet completely controllable environment. One key finding was that there may also be physical barriers to cell integration within decellularized tissues if used for support of vascularisation. Endothelial cells could be seeded via the

vasculature, but HDF functioned best when introduced via the organs lumen, in common with approaches optimized for heart and lung where cells where non-endothelial cells were introduced via the ventricle and alveolar space respectively [27,28]. This suggests the vasculature matrix may present a barrier that limits migration of HDF into the stroma or perivascular niche of the decellularized tissue.

There are clearly limitations in any in vitro study no matter how sophisticated a 3D model as it is unlikely to capture the physiological complexity of the in vivo situation. It is difficult for example to relate perfusion in vitro to in vivo. In this study we have made no attempt to consider transmural flow. Transmural flow is the perpendicular flow rate into the parenchyma. As blood travels along a vessel some fluid, interstitial fluid, will travel through to the parenchyma. This is important in delivering nutrients to adjacent cells. We have not attempted to calculate the proportion of flow that continues onto the further vessels and that which is incorporated into the transmural flow.

Another major challenge in the future will be to extend this to a more complex model which includes immune cells.

Other excellent studies of recellularised animal vascular nets from the Mertsching group have shown patency of such vascular nets repopulated with porcine cells and then implanted in pigs [35] and of a vascular net repopulated with human cells and implanted in a patient [36].

In conclusion, this work shows that an acellular matrix that retains the vascular patency and major ECM components of the native rat intestine can be produced via decellularization. Upon recellularization cells attach well, redistribute themselves thoroughly throughout the vascular network and show evidence of angiogenic

sprouting under perfusion conditions. This model not only has the ability to support cells but it also combines ECM components and the ability to perfuse cells under varying conditions. We suggest that this provides a valuable platform in which angiogenesis can be studied in vitro, meeting the growing need for 3D models which can be used to study complex systems which by definition cannot be readily studied in man or animals and to produce in vitro models which reduce animal experimentation.

Acknowledgements

We gratefully acknowledge the EPSRC Doctoral Training Centre in Tissue Engineering and Regenerative Medicine for funding this work via support of LD. Special thanks go to Julio Bissoli for his guidance with the intestine resection and cannulation and Giulia Gigliobianco for help with the CAM model.

Author Disclosure:

The authors declare no conflicts of interest.

References

[1] Fuchs JR, Nasseri BA, Vacanti JP. Tissue engineering: A 21st century solution to surgical reconstruction. Annals of Thoracic Surgery. 2001;72:577-91.

[2] Atala A. Tissue engineering and regenerative medicine: Concepts for clinical application. Rejuvenation Research. 2004;7:15-31.

[3] Griffith CK, Miller C, Sainson RCA, Calvert JW, Jeon NL, Hughes CCW, et al. Diffusion limits of an in vitro thick prevascularized tissue. Tissue Engineering. 2005;11:257-66.

[4] Novosel EC, Kleinhans C, Kluger PJ. Vascularization is the key challenge in tissue engineering. Advanced Drug Delivery Reviews. 2011;63.

[5] Kannan RY, Salacinski HJ, Sales K, Butler P, Seifalian AM. The roles of tissue engineering and vascularisation in the development of micro-vascular networks: a review. Biomaterials. 2005;26:1857-75.

[6] Rouwkema J, Rivron NC, van Blitterswijk CA. Vascularization in tissue engineering. Trends in Biotechnology. 2008;26:434-41.

[7] Carmeliet P, Jain RK. Molecular mechanisms and clinical applications of angiogenesis. Nature. 2011;473:298-307.

[8] Potente M, Gerhardt H, Carmeliet P. Basic and Therapeutic Aspects of Angiogenesis. Cell. 2011;146:873-87.

[9] Chung AS, Ferrara N. Developmental and Pathological Angiogenesis. In: Schekman R, Goldstein L, Lehmann R, editors. Annual Review of Cell and Developmental Biology, Vol 27. Palo Alto: Annual Reviews; 2011. p. 563-84.

[10] Sarig U, Au-Yeung GCT, Wang Y, Bronshtein T, Dahan N, Boey FYC, et al. Thick Acellular Heart Extracellular Matrix with Inherent Vasculature: A Potential Platform for Myocardial Tissue Regeneration. Tissue Engineering Part A. 2012;18:2125-37.

[11] Uygun BE, Soto-Gutierrez A, Yagi H, Izamis ML, Guzzardi MA, Shulman C, et al. Organ reengineering through development of a transplantable recellularized liver graft using decellularized liver matrix. Nature Medicine. 2010;16:814-U120.

[12] Reddy GK, Enwemeka CS. A simplified method for the analysis of hydroxyproline in biological tissues. Clinical Biochemistry. 1996;29:225-9.

[13] Rhaleb NE, Peng HM, Harding P, Tayeh M, LaPointe MC, Carretero OA. Effect of N-acetyl-seryl-aspartyl-lysyl-proline on DNA and collagen synthesis in rat cardiac fibroblasts. Hypertension. 2001;37:827-32.

[14] Farndale RW, Buttle DJ, Barrett AJ. Improved Quantitation And Discrimination Of Sulfated Glycosaminoglycans By Use Of Dimethylmethylene Blue. Biochimica Et Biophysica Acta. 1986;883:173-7.

[15] MacNeil S. Progress and opportunities for tissue-engineered skin. Nature. 2007;445:874-80.

[16] Pourageaud F, De Mey JG. Structural properties of rat mesenteric small arteries after 4-wk exposure to elevated or reduced blood flow. Am J Physiol. 1997;223(4):1699-706.

[17] Benedito R, Roca C, Sorensen I, Adams S, Gossler A, Fruttiger M et al. The notch ligans DII4 and Jagged1 have opposing effects on angiogenesis. Cell. 2009;137(6):1124-35

[18] Lobov IB1, Renard RA, Papadopoulos N, Gale NW, Thurston G, Yancopoulos GD, Wiegand SJ. Delta-like ligand 4 (Dll4) is induced by VEGF as a negative regulator of angiogenic sprouting." Proceedings of the National Academy of Sciences 2007;104(9):3219-3224.

[19] Geudens I, Gerhardt H. Coordinating cell behaviour during blood vessel formation. Development. 2011;138(21):4569-83.

[20] Pedrosa AR, Trindade A, Fernandes AC, Carvalho C, Gigante J, Tavares AT et al. Endothelial Jagged1 antagonizes Dll4 regulation of endothelial branching and

promotes vascular maturation downstream of Dll4/Notch1. Arterioscler Thromb Vasc Biol. 2015;35(5):1134-46

[21] Jakobsson L, Franco CA, Bentley K, Collins RT, Ponsioen B, Aspalter IM et al. Endothelial cells dynamically compete for the tip cell position during angiogenic sprouting. Nature Cell Biology. 2010;12:943–953

[22] Beets K, Huylebroeck D, Moya IM, Umans L, Swijsen A. Robustness in angiogenesis: Notch and BMP shaping waves. Trends in Genetics. 2013;29(3):140-149.

[23] Atala A, Bauer SB, Soker S, Yoo JJ, Retik AB. Tissue-engineered autologous bladders for patients needing cystoplasty. Lancet. 2006;367:1241-6.

[24] Bhargava S, Patterson JM, Inman RD, MacNeil S, Chapple CR. Tissue-engineered buccal mucosa urethroplasty - Clinical outcomes. European Urology. 2008;53:1263-71.

[25] Macchiarini P, Jungebluth P, Go T, Asnaghi MA, Rees LE, Cogan TA, et al. Clinical transplantation of a tissue-engineered airway. Lancet. 2008;372:2023-30.

[26] Staton CA, Reed MWR, Brown NJ. A critical analysis of current in vitro and in vivo angiogenesis assays. International Journal of Experimental Pathology. 2009;90:195-221.

[27] Ott HC, Matthiesen TS, Goh SK, Black LD, Kren SM, Netoff TI et al. Perfusion-decellularized matrix: using nature's platform to engineer a bioartificial heart. Nature medicine. 2008;14(2): 213-221.

[28] Petersen TH, Calle EA, Zhao L, Lee EJ, Gui L, Raredon MB et al. Tissue-engineered lungs for in vivo implantation. Science. 2010;329(5991):538-541.

[29] Grinnell F, Feld MK. Initial adhesion of human fibroblasts in serum-free

medium: possible role of secreted fibronectin. Cell. 1979;17(1):117-129.

[30] McKeown-Longo PJ, Mosher DF. Binding of plasma fibronectin to cell layers of human skin fibroblasts. J Cell Biol. 1983;97(2):466-72

[31] Wragg JW, Durant S, McGettrick HM, Sample KM, Egginton S, Bicknell R. Shear stress regulated gene expression and angiogenesis in vascular endothelium. Microcirculation. 2014;290-300.

[32] Li H, Chang J. Bioactive silicate materials stimulate angiogenesis in fibroblast and endothelial cell co-culture system through paracrine effect. Acta Biomaterialia. 2013;9:6981-91.

[33] Stevens KR, Kreutziger KL, Dupras SK, Korte FS, Regnier M, Muskheli V, et al. Physiological function and transplantation of scaffold-free and vascularized human cardiac muscle tissue. Proceedings of the National Academy of Sciences of the United States of America. 2009;106:16568-73.

[34] Hurley JR, Balaji S, Narmoneva DA. Complex temporal regulation of capillary morphogenesis by fibroblasts. American Journal of Physiology-Cell Physiology. 2010;299:C444-C53.

[35] Schanz J, Pusch J, Hansmann J, Walles H. Vascularised human tissue models: A new approach for the refinement of biomedical research.

[36] Mertsching H, Schanz J, Steger V, Schandar M, Schenk M, Hansmann J, et al. Generation and transplantation of an autologous vascularised bioartificial human tissue. Transplantation. 2009;88:203-210

Reprint Author: S. MacNeil

Figure Legends

Figure 1. Decellularized intestine maintains vascular patency. Macroscopic view of fresh intestine region of intestine (**A**) and decellularized intestine after treatment with detergent (**B**). Scale bars are 10mm. **C.** Macroscopic view of defined vascular channels remaining after decellularization. Scale bar is 5mm. **D.** Evidence of vascular channel patency after the intestine is infused with blue food dye. Scale bar is 5mm. **E.** Microscopic evidence of vascular channel patency after infusion with FITC-Dextran. Scale bar is 200 μm.

Figure 2. Characterisation of the nucleic acid and extracellular matrix content of decellularized intestine. **A.** Histological staining of nuclei and extracellular matrix content of intact and decellularized intestine. Nuclei were visualised by staining with haematoxylin and eosin or DAPI using light or fluorescence microscopy respectively. Scale bars are 200 μm. Picosirius red staining was used to stain collagen fibres under white light and then imaged under polarised light to detect differences in fibrilar collagen content. Glycosaminoglycans (GAG) and mucinous polysaccharises (MPS) were detected by staining with Alcian Blue. Scale bars are 200 μm. **B.** Quantification of DNA, Collagen-I and GAG content. DNA was quantified after extraction from intact and decellularized intestine by measuring absorbance at 260 nm. Error bars are ± SEM. $N = 3$, $p < 0.0001$. Collagen content was estimated after acid extraction and quantification of 4-hydroxy-proline content. Error bars are ± SEM. $N = 3$ and $p < 0.05$. **I –**Quantification of GAG in tissue extracts was performed using the dimethylmethylene blue (DMB) assay. Error bars are ± SEM. $N = 3$, $p > 0.05$.

Figure 3. Characterisation of elastin, laminin and fibronectin content in decellularized intestine. **A - B.** Verhoeff Van Gieson staining of FFPE sections of intestine for elastin before (A) and after (B) decellularization. Scale bar is 200 μm. **C – D.** Immunofluorescence staining of frozen sections of intestine before (C) and after (D) decellularization for pan-laminin (red) and counterstained with DAPI (blue). Scale bar is 50 μm. **E – F.** Immunofluorescence staining of fibronectin (red) and nuclei (DAPI, blue) before and after decellularization. Scale bar is 50 μm.

Figure 4. Decellularized intestine retains the capacity to induce neo-vascularisation in the CAM assay. Example photographs of CAM after 7 days post implantation of a collagen I gel (**A,** negative control) and decellularized intestine (**B**). The position of the collagen gel and intestine is highlighted by the dashed circle. Scale bar is 2mm. **C.** Quantification of blood vessels converging towards the implanted material. Error bars are ± SEM. N = 3, $p < 0.0001$.

Figure 5 . Retention of viable human ECs in the vascular channels of decellularized intestine is dependent on perfusion flow rate. The decellularized intestine was perfused via the vasculature with HDMEC then cultured for 24 hours in the absence of perfusion (24h STATIC), 72 hours without perfusion (72h STATIC) or for 72 hours with perfusion at 2.7, 0.5 or 0.025 ml/min. After the times indicated the intestine was sectioned and stained to distinguish between LIVE/DEAD cells using propidium iodide and Syto 9 (Left column). Live cells are shown in green and non-viable cells shown in red. Alternatively the intestine was stained to detect HDMEC after fixing at the indicated times using an immunofluorescence whole-

mount staining method with anti-CD31 (red) and DAPI (nuclei, blue). Scale bars are 100 μm.

Figure 6. Retention of viable human ECs in the vascular channels of decellularized intestine is increased by continuous perfusion and human fibroblasts. The decellularized intestine was perfused via the vasculature with HDMEC (top row), or HDMEC and HDF (middle row), or the vasculature perfused with HDMEC and the intestine lumen perfused with HDF (bottom row). The intestine was then cultured for 24 hours in the absence of perfusion (24h STATIC), 72 hours without perfusion (72h STATIC) or for 72 hours with perfusion at 0.025 ml/min. After the times indicated the intestine was sectioned and stained to distinguish between LIVE/DEAD cells using propidium iodide and Syto 9. Live cells are shown in green and non-viable cells shown in red. Scale bars are 100 μm.

Figure 7. Human ECs form a continuous monolayer within decellularized intestine in the presence of perfusion and human fibroblasts. **A.** Intestine was re-populated with HDMEC with or without HDF as described in Fig 6 before fixing at the times indicated after perfusion of the vascular channels with HDMEC alone, with HDF the vascular channels or with HDMEC in the vascular channels and HDF through the intestinal lumen. The intestine was stained after fixing at the indicated times using an immunofluorescence whole-mount staining method with anti-CD31 (red) and DAPI (nuclei, blue). Scale bars are 100 μm. **B.** Larger scale images of intestine with HDMEC perfused through the vascular channel and HDF perfused through the intestinal lumen after staining for CD31 and nuclei (DAPI, blue). Scale bars are 100 and 50μm.

Figure 8. The engineered vasculature within the decellularized intestine maintains the capacity for sprouting angiogenesis. HDMEC were perfused via the vascular channels and HDF were seeded via the intestinal lumen as described in Fig 6 and 7 before perfusion at 0.025 ml/min for 72 hours. Collagen gels with or without VEGFA were placed on top of the intestine. Intestine sections were fixed and stained for CD31 or Dll4 using immunofluorescence whole mount staining methods. Example images are shown of intestine with and without VEGFA and regions positive for Dll4 are indicated by arrows. Scale bars are 100 μm.

Figure 1:

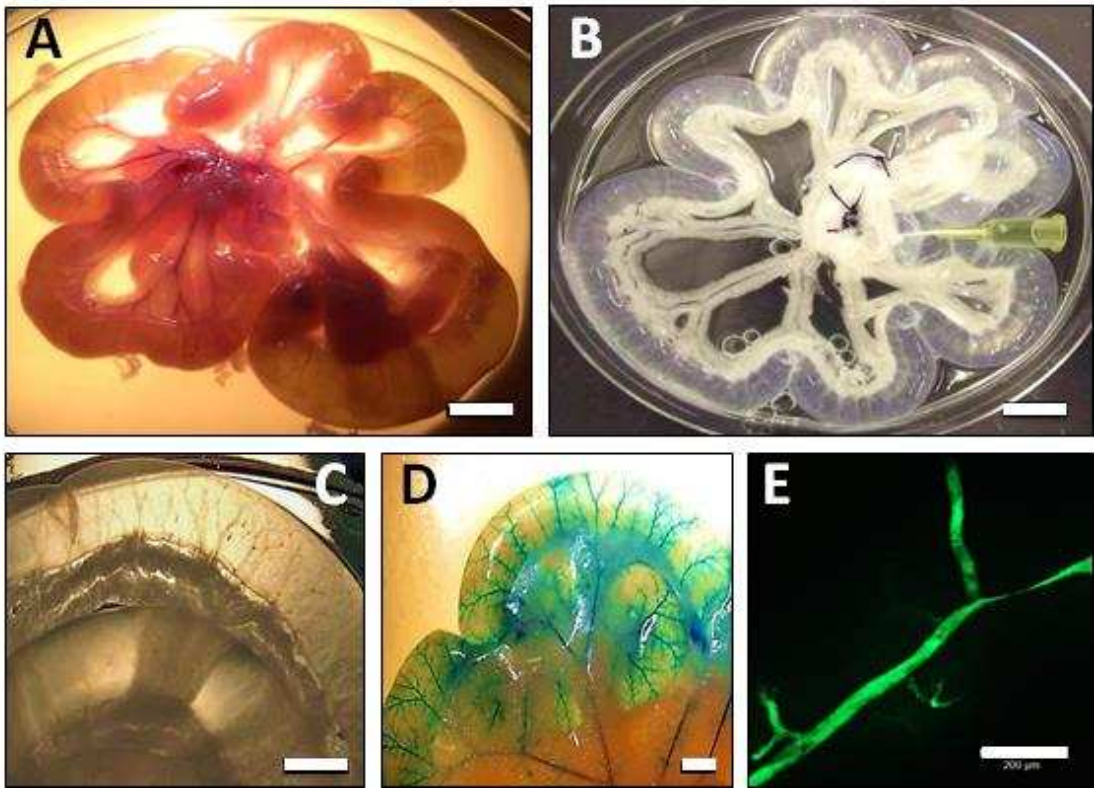

Figure 2:

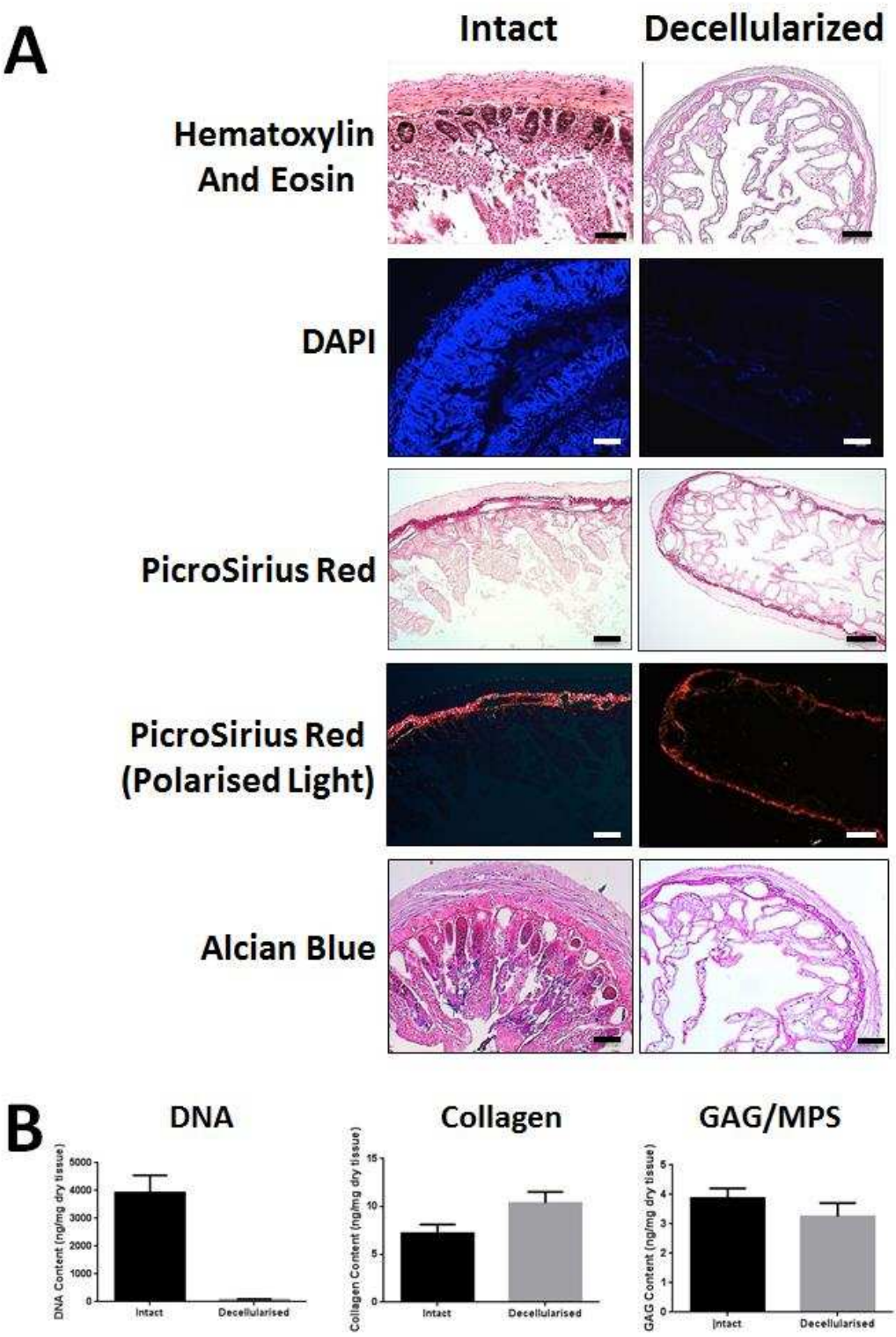
A
Intact
Decellularized
Hematoxylin And Eosin
DAPI
PicroSirius Red
PicroSirius Red (Polarised Light)
Alcian Blue
B
DNA
DNA Content (ng/mg dry tissue)
5000
4000
3000
2000
1000
0
Intact
Decellularised
Collagen
Collagen Content (ng/mg dry tissue)
15
10
5
0
Intact
Decellularised
GAG/MPS
GAG Content (ng/mg dry tissue)
5
4
3
2
1
0
Intact
Decellularised

Figure 3:

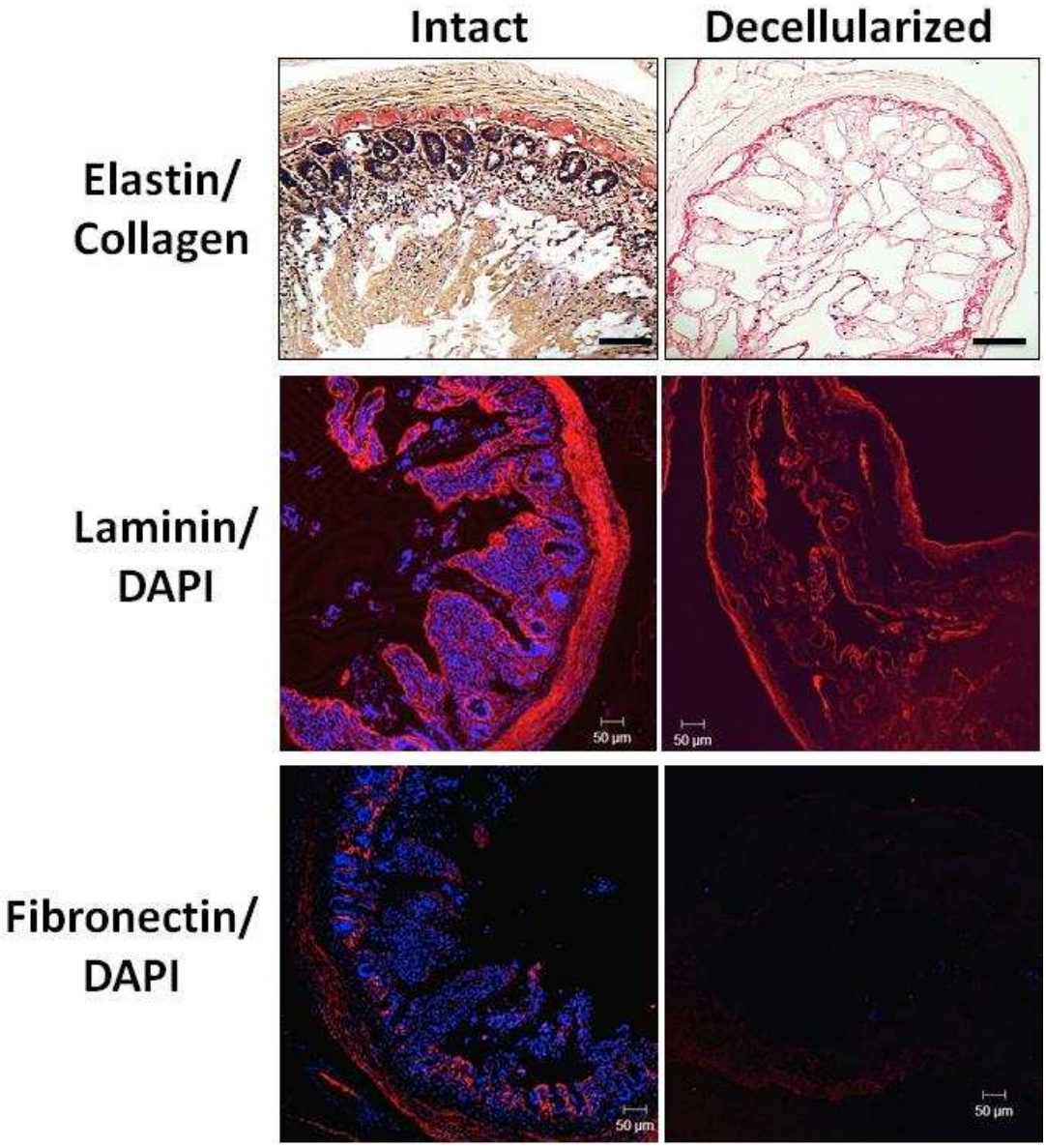
Intact
Decellularized
Elastin/
Collagen
Laminin/
DAPI
Fibronectin/
DAPI
50 µm
50 µm
50 µm
50 µm

Figure 4:

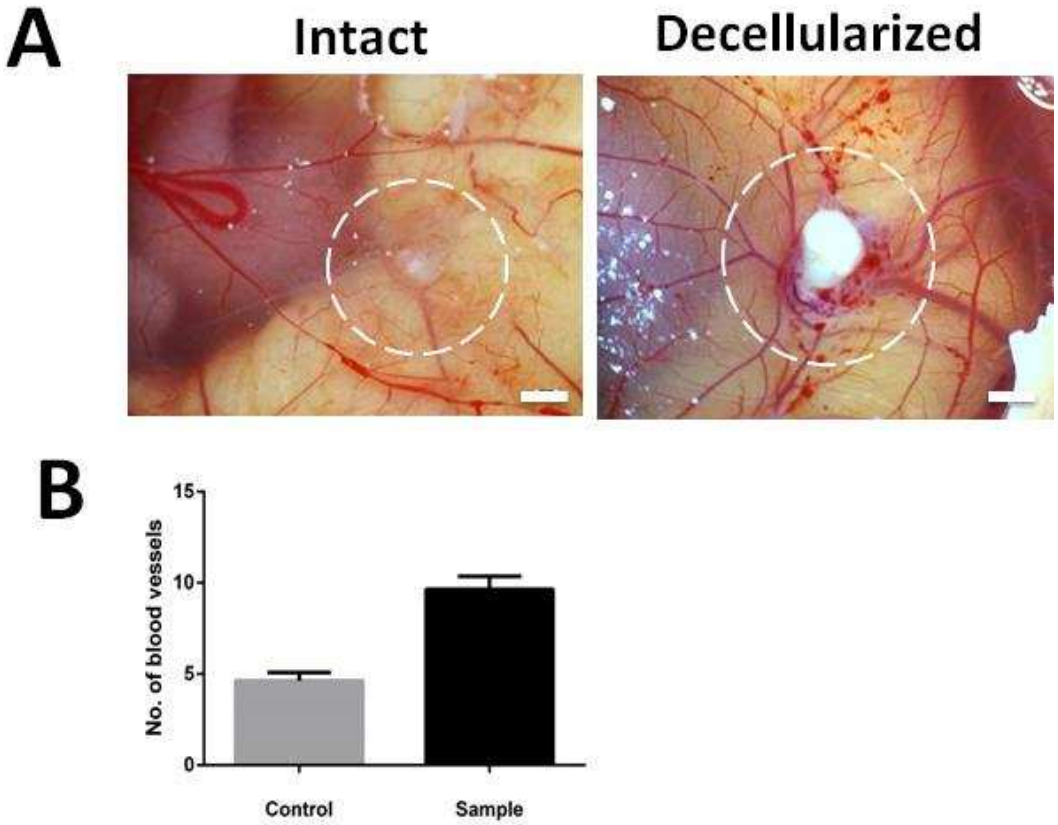
A
Intact
Decellularized
B
No. of blood vessels
15
10
5
0
Control
Sample

Figure 5:

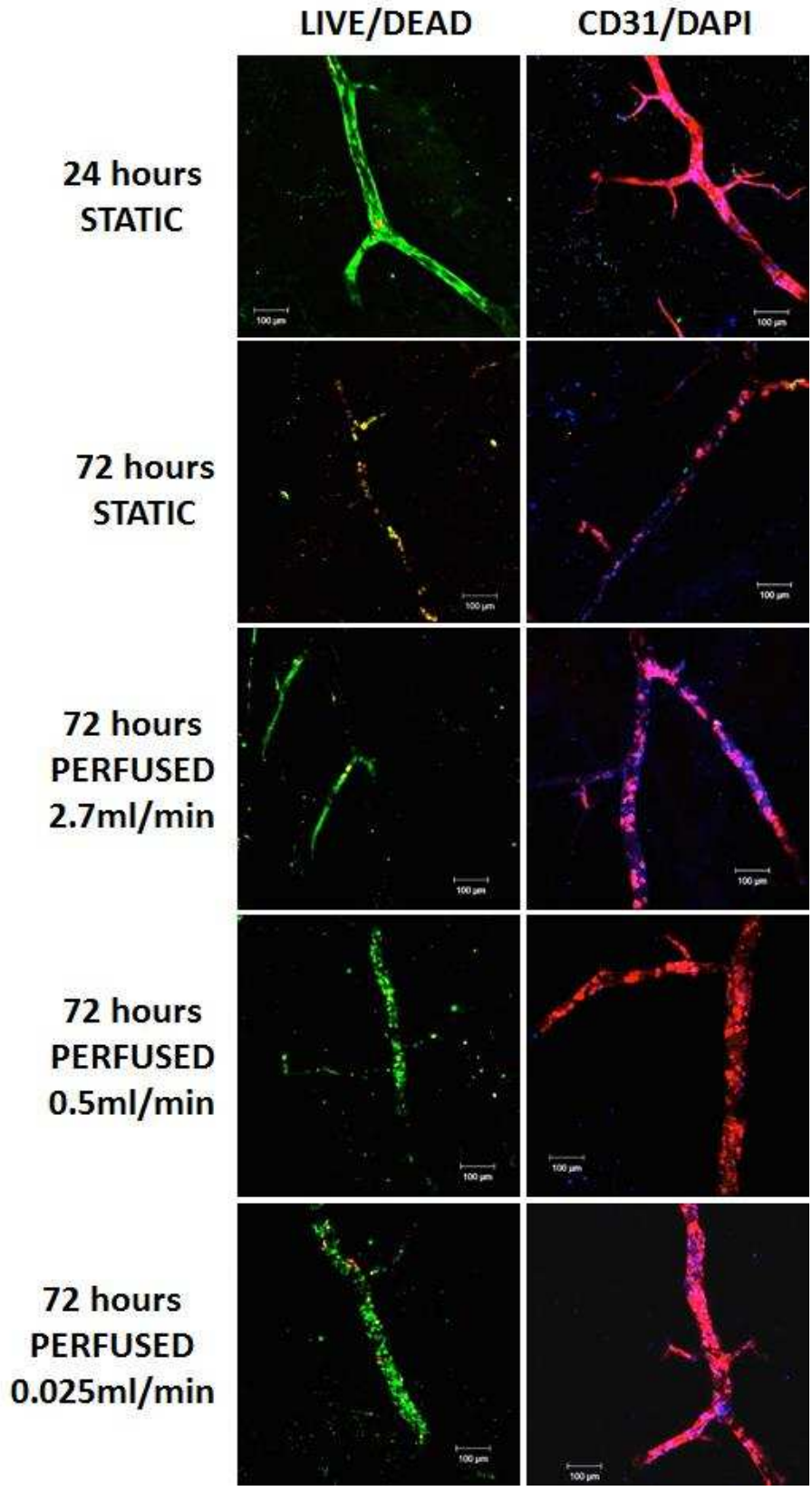
LIVE/DEAD
CD31/DAPI
24 hours STATIC
72 hours STATIC
72 hours PERFUSED 2.7ml/min
72 hours PERFUSED 0.5ml/min
72 hours PERFUSED 0.025ml/min

Figure 6:

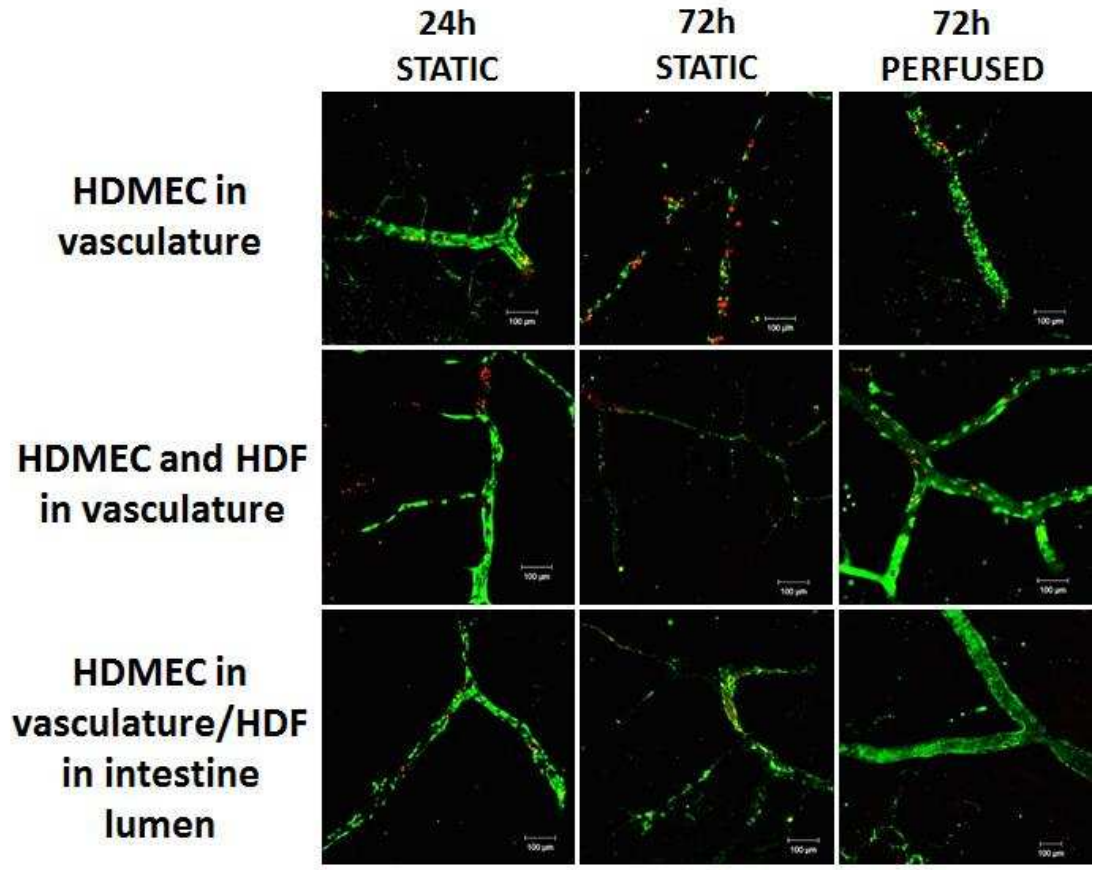
24h
STATIC
72h
STATIC
72h
PERFUSED
HDMEC in vasculature
HDMEC and HDF in vasculature
HDMEC in vasculature/HDF in intestine lumen

Figure 7:

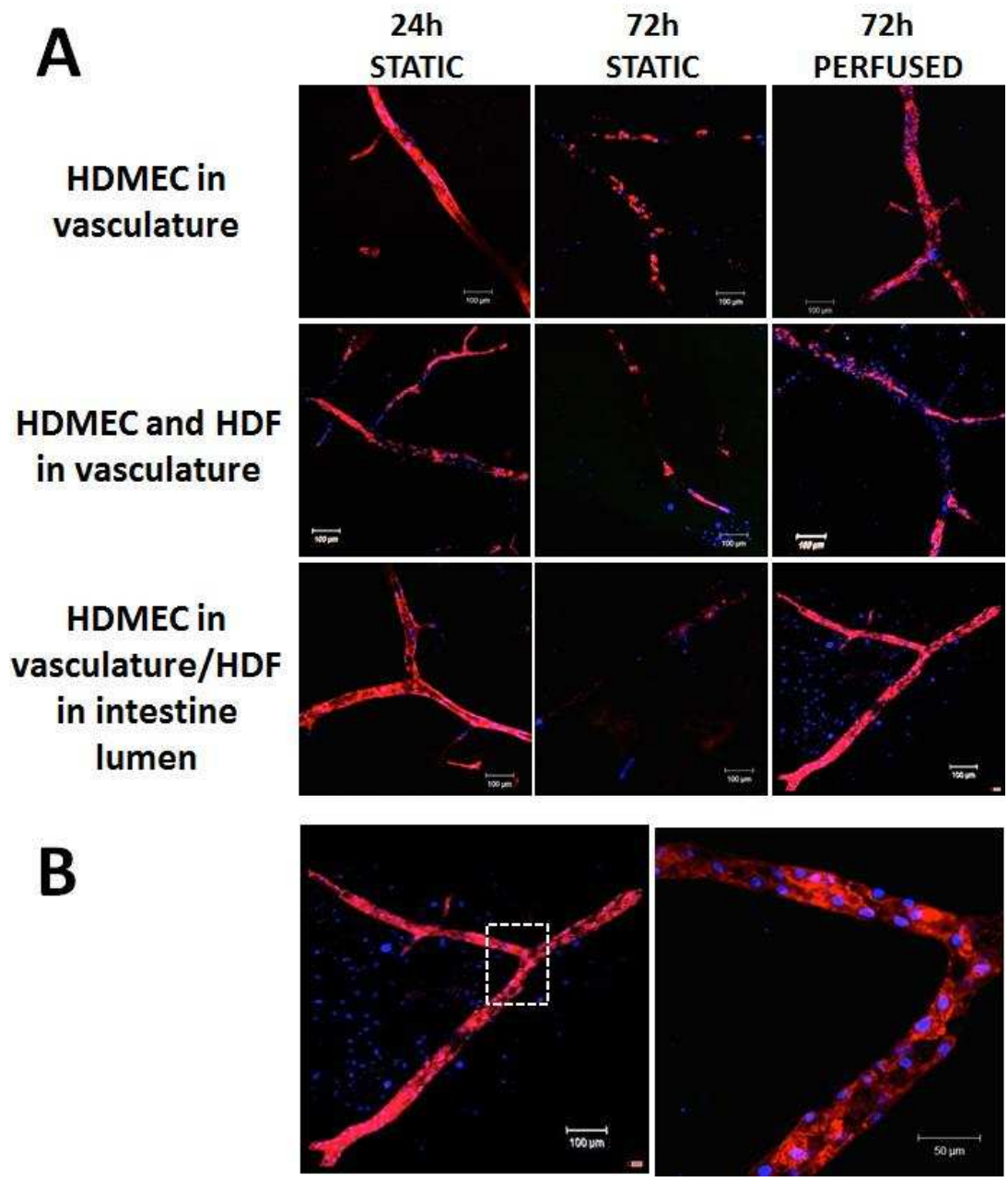
A
24h STATIC
72h STATIC
72h PERFUSED
HDMEC in vasculature
HDMEC and HDF in vasculature
HDMEC in vasculature/HDF in intestine lumen
B
100 µm
50 µm

Figure 8:

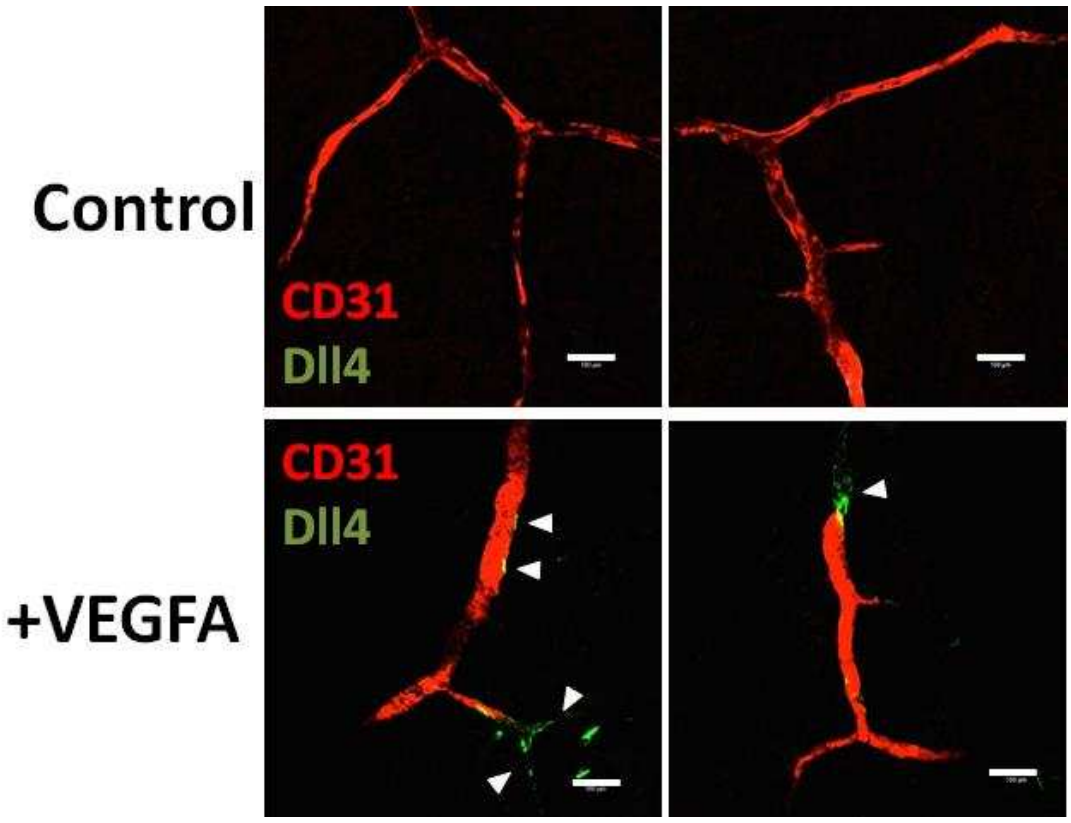

Table 1: Assessment of extent of endothelialisation in jejunum with addition of HDFs and flow

Expt No	+HDFs	Static		Perfused (rate ml/min)	
		1 day	3 days	3 days	
1	0	+++	ND	ND	
2	0	++	+	++	(2.7 ml/min)
3	0	+++	+	++	(2.7 ml/min)
4	+HDF (vessel)	++	+	++	(0.025 ml/min)
5	+HDF (lumen)	+++	0	+++	(0.025 ml/min)
6	0	ND	ND	++	(0.025 ml/min)
	+HDF (vessel)	ND	ND	+	(0.025 ml/min)
	+HDF (lumen)	ND	ND	+++	(0.025 ml/min)

The presence of endothelial cells was detected using immunostaining for CD31 and photographs were then scored by three observers blind to the nature of the experiment. Observers were asked to score 0 for no evidence of endothelial cell cover, + for some endothelial cells but poor (less than 25% cover), ++ reasonable but incomplete endothelial cover, +++ complete endothelial cover.